Kinetics and mechanisms of the reactions of the electrogenerated tetramethoxythianthrene cation radical and dication with methanol and pyridine derivatives in acetonitrile

Munetaka Oyama,*† Teruo Sasaki and Satoshi Okazaki*

Department of Material Chemistry, Graduate School of Engineering, Kyoto University,
Sakyo-ku, Kyoto, 606-8501, Japan. E-mail: oyama@mc.kyoto-u.ac.jp; Fax: +81-75-761-8846;
Tel: +81-75-753-5885

Received (in Cambridge, UK) 15th September 2000, Accepted 3rd April 2001
First published as an Advance Article on the web 3rd May 2001

In order to clarify the differences in reactivity between cation radicals and dications, the kinetics and mechanisms were analysed in detail for the reactions of the electrogenerated 2,3,7,8-tetramethoxythianthrene cation radical ($TMT^{\bullet+}$) and of the dication (TMT^{2+}) with methanol and pyridine derivatives by using a pulse-electrolysis stopped-flow method. From the rate law determined for each reaction, the reaction mechanisms were elucidated, though they are different depending on the couples in the reactions. The reactions of $TMT^{\bullet+}$ proceeded by multi-step reactions including the electron transfer of another $TMT^{\bullet+}$ to generate TMT before the rate-determining step (rds). In contrast, in the reactions of TMT^{2+}, it was found that the rds was the first or the second step of the reaction; *i.e.* the unstable cationic intermediate seems to be formed directly, not by the electron transfer. In addition to the excessive charge present in the dicationic state, a mechanism in which TMT^{2+} is easily accessible to the rds also seems to explain the high reactivity of TMT^{2+}. The differences in the reaction mechanism depending on the nucleophiles were also supported by observing the substituent effects of pyridine derivatives on the reactions.

Introduction

While numerous studies have been devoted to the kinetic analysis of electrogenerated cation radicals with nucleophiles,[1–3] little is known about the reaction kinetics of electrogenerated dications.[4,5] For the purpose of clarifying the comprehensive reactivity of electrogenerated species, it would be valuable to compare the reaction kinetics and mechanisms for cation radicals and dications. In addition, because the dicationic species has previously been thought to be produced by a disproportionation reaction of the cation radicals,[6] experimental discrimination of both reactions is necessary to elucidate the reactivity of the electrogenerated species.

However, the kinetic analysis of dications has been very difficult mainly because dications are generally too unstable to be detected. Another problem is the comproportionation reaction between a dication and its neutral molecule to generate two cation radicals, which would cause significant interference in the analysis of the pure reaction kinetics of dications with nucleophiles.

In a previous communication, we analysed the reactions of electrogenerated 2,3,7,8-tetramethoxythianthrene (TMT) dication (TMT^{2+}) and cation radical ($TMT^{\bullet+}$) with nucleophiles using a pulse-electrolysis stopped-flow method.[7] Owing to its methoxy substituents, TMT^{2+} is stable enough in acetonitrile (AN).[8] Therefore, the column electrolysis method, in which exhaustive electrolysis can be achieved,[9] permits us to analyse the reactions of electrogenerated TMT^{2+} and to compare those with the reactions of $TMT^{\bullet+}$. As a result, the changes in the reaction mechanisms were demonstrated in addition to the differences in the reaction rates.

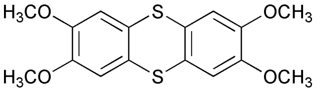

In the present paper, the kinetics and mechanisms of the reactions of TMT^{2+} and $TMT^{\bullet+}$ with various nucleophiles are reported in detail. As nucleophiles, methanol (MeOH), pyridine (Py) and pyridine derivatives (XPy) are examined in this comprehensive study.

The reactions of cation radicals with Py have been investigated in detail, in particular, those of the 9,10-diphenylanthracene cation radical ($DPA^{\bullet+}$).[1–3] However, because of the high reactivity of the thianthrene cation radical ($TH^{\bullet+}$) toward Py, compared with that of $DPA^{\bullet+}$, there has been little study of the reaction of $TH^{\bullet+}$ with Py.[10] The lower reactivity of $TMT^{\bullet+}$ compared with $TH^{\bullet+}$ permitted analysis of the kinetics and mechanisms of its reaction with Py,[7,11] and, furthermore, the reactions of TMT^{2+} with nucleophiles can be investigated thoroughly owing to the even lower reactivity of TMT^{2+}.

Through the comprehensive analysis of their reactions with nucleophiles the aim of this paper is to show how different are the reaction kinetics and mechanisms for the dication and cation radical in the case of a model compound, TMT.

Experimental

Analysis of reaction kinetics and mechanisms

The details of spectroscopic measurements using the pulse-electrolysis stopped-flow method have been described previously.[12,13] In the present work, the solution of TMT^{2+} or $TMT^{+\bullet}$, which was quantitatively prepared by a controlled-potential electrolysis, was mixed with a solution containing nucleophiles (MeOH, Py or XPy), and then the changes in absorption

---

† *Present address*: International Innovation Center, Kyoto University, Sakyo-ku, Kyoto 606-8501, Japan.

DOI: 10.1039/b007497g

spectra with time or the time–decay curves of absorbance at a fixed wavelength were observed in an optical flow-cell. The temperature was controlled at 25 °C by circulating water on the outside of the cell. Electrolysis was performed with a PAR Model 173 potentiostat.

Electrochemical analysis

Cyclic voltammograms (CV) were measured using a PAR 174 analyser. A Pt disk electrode of 1.0 mm diameter was used as the working electrode. The reference electrode used was the Pt | (I_3^-, I^-) in AN. All CV experiments were performed in an H-shaped cell at *ca.* 25 °C.

Product analysis was carried out using a batchwise controlled-potential electrolysis of TMT in the presence of nucleophiles using a platinum mesh working electrode for the stirred solution as reported previously.[13] The isolated product was identified by means of NMR and MS.

Reagents

Acetonitrile (AN, Nacalai Tesque, GR grade) was twice distilled over P_2O_5. The supporting electrolyte, tetrabutylammonium perchlorate (TBAP), was made from sodium perchlorate and tetrabutylammonium bromide, and purified by recrystallization five times from ethanol–water. Methanol and pyridine derivatives (Aldrich, Wako Chemicals, or Nacalai Tesque) were used as received. TMT was prepared from 1,2-dimethoxybenzene and SCl_2 following the procedure described in the literature.[14]

Results and discussion

Electrochemical and spectroscopic properties of TMT^{2+} and $\mathrm{TMT}^{\cdot+}$

At first, the cyclic voltammogram of TMT in AN was measured. Owing to its methoxy substituents, TMT^{2+} is rather stable in AN and two reversible waves are observed in the cyclic voltammogram even at a scan rate of 100 mV s^{-1} as shown in Fig. 1A.

Because both of the electrooxidized states are stable, we observed the absorption spectra of $\mathrm{TMT}^{\cdot+}$ and TMT^{2+} in AN using the electrolysis stopped-flow method. By applying potentials of 0.85 or 1.25 V to the column electrode for 10 s, and delivering the solution into the optical cell by means of a piston drive, the absorption spectra of $\mathrm{TMT}^{\cdot+}$ and TMT^{2+} could be easily observed selectively as shown in Fig. 1B, C.

At the wavelengths of both absorption maxima, the changes in absorbance depending on the applied potential were measured, the result of which is shown in Fig. 2. The plateau values are observed in the potential regions corresponding to the generation of $\mathrm{TMT}^{\cdot+}$ and TMT^{2+}. In addition, for the observed results in the potential region around 1.0 V, a Nernstian response was confirmed for the concentrations of $\mathrm{TMT}^{\cdot+}$ and TMT^{2+}. Thus, quantitative electrolysis was ascertained in the present method.

On the basis of these results and the plateau values, the molar absorptivity was determined to be 9.8×10^3 M^{-1} cm^{-1} at 800 nm for $\mathrm{TMT}^{\cdot+}$ and 3.0×10^4 M^{-1} cm^{-1} at 701 nm for TMT^{2+}, respectively. While the value of the molar absorptivity of TMT^{2+} was previously reported to be comparable ($\log \varepsilon = 4.15$) to that of $\mathrm{TMT}^{\cdot+}$ ($\log \varepsilon = 4.00$),[15] we have used the value of 3.0×10^4 M^{-1} cm^{-1} in further analysis on the basis of our qualified result.

Because it was found that TMT^{2+} and $\mathrm{TMT}^{\cdot+}$ could be generated quantitatively and selectively with this method, next, the reaction processes with nucleophiles were traced by mixing the AN solutions of TMT^{2+} or $\mathrm{TMT}^{\cdot+}$ and nucleophiles directly using the pulse-electrolysis stopped-flow method.

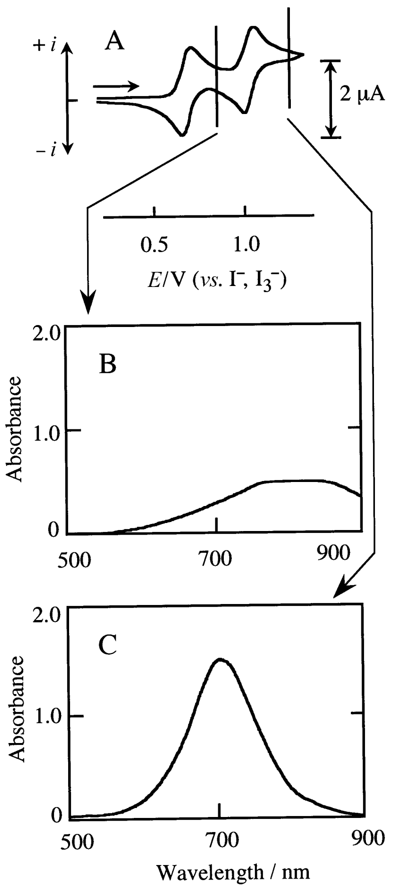

Fig. 1 (A) Cyclic voltammogram of TMT in AN and (B, C) absorption spectra of the oxidized solutions of TMT. (A) Working electrode: platinum disk electrode (diam. 1.0 mm). Reference electrode: Pt | (I^-, I_3^-) electrode. Scan rate: 100 mV s^{-1}. (B, C) Absorption spectra measured using the pulse-electrolysis stopped-flow method at the applied potential of 0.85 (B) and 1.25 V (C), which are attributed to the spectra of $\mathrm{TMT}^{\cdot+}$ and TMT^{2+}, respectively.

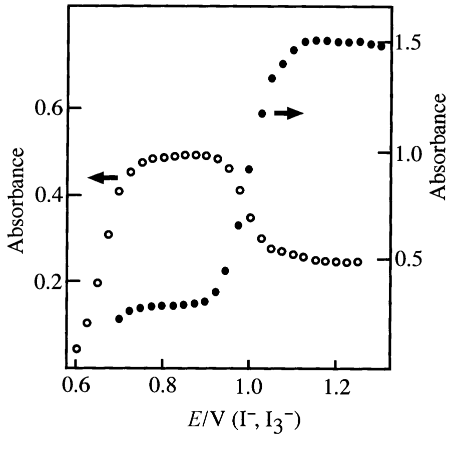

Fig. 2 Changes in absorbance depending on the applied potential measured using the pulse-electrolysis stopped-flow method. ○ At a wavelength of 800 nm, corresponding to the absorption maximum of $\mathrm{TMT}^{\cdot+}$. ● At a wavelength of 701 nm, corresponding to the absorption maximum of TMT^{2+}.

Reaction of TMT^{2+} with MeOH

Because the reaction with MeOH can be regarded as a prototypical reaction for water and alcohols,[13,16] we analysed the reactions of TMT^{2+} and $\mathrm{TMT}^{\cdot+}$ with MeOH.

Fig. 3A shows a typical result of the dynamic transformation of the absorption spectra in the reaction of TMT^{2+} with MeOH. This result clearly shows that TMT^{2+} decays monoton-

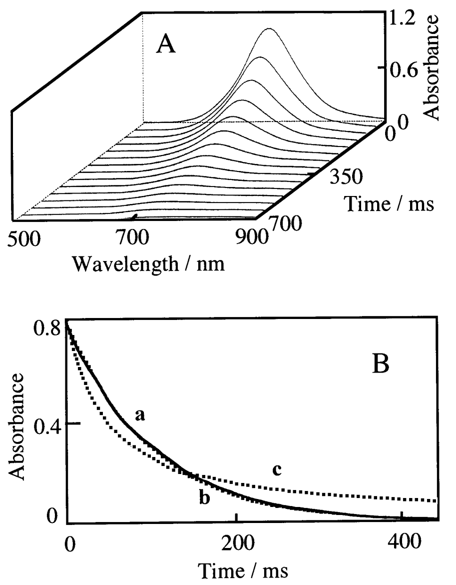

Fig. 3 (A) Dynamic transformation of the absorption spectra in the reaction of TMT^{2+} and MeOH. The solution of TMT^{2+} was produced by electrolyzing the AN solution of 0.50 mM TMT containing 0.1 M TBAP with the applied potential of 0.12 V for 10 s, and then it was mixed with the solution of 0.50 M MeOH (time intervals: 50 ms). (B) (a) Changes in absorbance with time at 701 nm, corresponding to the absorption maximum of TMT^{2+} in spectra (A); (b), (c) decay curves simulated assuming a first- and second-order reaction, respectively (dotted lines).

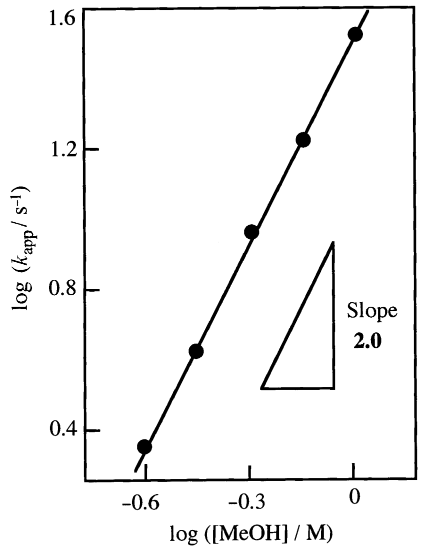

Fig. 4 Dependence of the pseudo-first-order rate constant, k_{app}, on the concentration of MeOH in the reaction of TMT^{2+} with MeOH.

ously without forming $TMT^{\bullet +}$. Namely, it is inferred that this reaction does not involve homogeneous electron transfer from TMT^{2+} to form a sufficient amount of $TMT^{\bullet +}$.

For the time–decay curve of TMT^{2+} at 701 nm [Fig. 3B(a)], numerical simulation analysis was performed as reported previously[13] on the basis of first- and second-order decays to yield curves (b) and (c) in Fig. 3B, respectively. As a result, it was clarified that the reaction was first order in TMT^{2+} from the excellent fit.

Given that the rate law of this reaction can be expressed by eqn. (1), several values of the pseudo-first-order rate constant, k_{app}, were measured by altering the concentration of MeOH.

$$-d[TMT^{2+}]/dt = k_{app}[TMT^{2+}] \qquad (1)$$

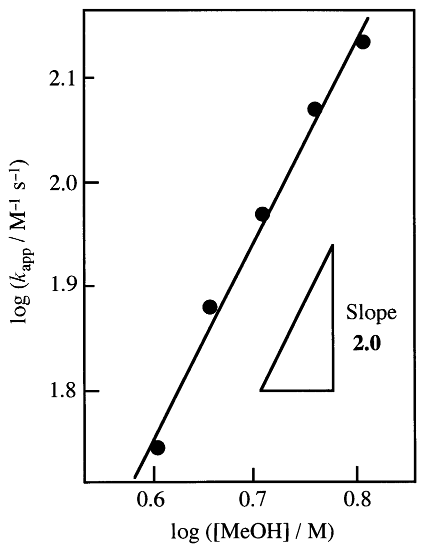

Fig. 5 Dependence of the pseudo-second-order rate constant, k_{app}, on the concentration of MeOH in the reaction of $TMT^{\bullet +}$ with MeOH.

As a consequence, the dependence of the k_{app} values on [MeOH] was obtained as shown in Fig. 4. From this relationship, the reaction order of MeOH was determined to be second, so that the rate law can be defined as given in eqn. (2).

$$-d[TMT^{2+}]/dt = k[TMT^{2+}][MeOH]^2 \qquad (2)$$

The rate constant, k, in eqn. (2) was determined to be 3.3 × 10 M^{-2} s^{-1}. The rate law represented by eqn. (2) means that the first encounter step between TMT^{2+} and MeOH [eqn. (3)] is in equilibrium and the proton abstraction by another MeOH [eqn. (4)] is the rate-determining step (rds).

$$TMT^{2+} + MeOH \rightleftharpoons TMT(MeOH)^{2+} \qquad (3)$$

$$TMT(MeOH)^{2+} + MeOH \xrightarrow[rds]{} TMT(MeO)^{+} + MeOH_2^{+} \qquad (4)$$

This mechanism is similar to that reported for the reaction of the 10-phenylphenothiazine dication with water.[4] In addition, the result that the cationic species, $TMT(MeO)^{+}$, is produced in the rds is similar to the reaction of $TH^{\bullet +}$ with water.[3] Because the isolated product in this reaction was only 2,3,7,8-tetramethoxythianthrene 5-oxide [TMT(O)], the reaction after eqn. (4) to produce TMT(O) is assumed to proceed rapidly in solution or in the work-up processes.

Reaction of $TMT^{\bullet +}$ with MeOH

Similarly, kinetic analysis was performed for the reactions of $TMT^{\bullet +}$ with MeOH. As a result of the simulation for the decay curves of $TMT^{\bullet +}$ at 800 nm after mixing with MeOH, it was ascertained that this reaction is second-order in $TMT^{\bullet +}$ [eqn. (5)].

$$-d[TMT^{\bullet +}]/dt = k_{app}[TMT^{\bullet +}]^2 \qquad (5)$$

Fig. 5 shows the plot of log k_{app} *vs.* log [MeOH]. From this relationship, the reaction order of MeOH was determined to be second. Hence, the rate law is expressed by eqn. (6), and the reaction mechanism can be summarized by eqns. (7)–(9). In addition, the rate constant, k, in eqn. (6) was determined to be 4.5 M^{-3} s^{-1}.

$$-d[TMT^{\bullet +}]/dt = k[TMT^{\bullet +}]^2[MeOH]^2 \qquad (6)$$

$$TMT^{\bullet +} + MeOH \rightleftharpoons TMT(MeOH)^{\bullet +} \qquad (7)$$

$$TMT(MeOH)^{\bullet +} + MeOH \rightleftharpoons TMT(MeO)^{\bullet} + MeOH_2^{+} \qquad (8)$$

$$TMT(MeO)^{\bullet} + TMT^{\bullet +} \xrightarrow[rds]{} TMT(MeO)^{+} + TMT \qquad (9)$$

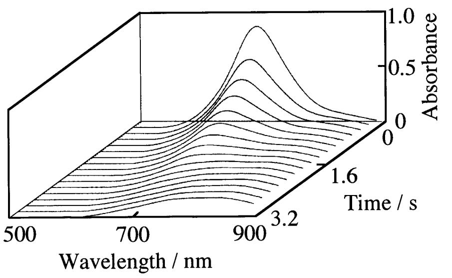

Fig. 6 Dynamic transformation of absorption spectra in the reaction of TMT^{2+} and Py. The solution of TMT^{2+} was produced by electrolyzing the AN solution of 0.50 mM TMT containing 0.1 M TBAP with the applied potential of 0.12 V for 10 s, and then it was mixed with the solution of 2.5 mM MeOH. Time interval: 200 ms.

From a mechanistic aspect, the possibility of a disproportionation reaction of $TMT^{\bullet+}$ [eqn. (10)] can be ruled out

$$TMT^{\bullet+} + TMT^{\bullet+} \underset{}{\overset{K_{dis}}{\rightleftharpoons}} TMT^{2+} + TMT \qquad (10)$$

using the values determined in this work, as described previously.[3]

That is, on the basis of the difference in the formal potentials, the disproportionation constant of eqn. (10) (K_{dis}) can be estimated to be $10^{-6.7}$. If the reaction of $TMT^{\bullet+}$ proceeds *via* the disproportionation and the follow-up reactions of eqns. (3) and (4), the reaction rate should be expressed as 2 $K_{dis}k$. Because the value of k was 33 M^{-2} s^{-1}, as determined above, the contribution of the disproportionation reaction can be concluded to be very small, if anything. This means that $TMT^{\bullet+}$ surely reacts with MeOH in the first stage of the reaction as in eqns. (7)–(9), as is usual in the nucleophilic reactions of cation radicals.[3,6]

From a comparison of eqns. (7)–(9) with the reaction of TMT^{2+} in eqns. (3) and (4), it can be concluded that the reaction of $TMT^{\bullet+}$ with MeOH involves one more equilibrium before the rds. However, the formation of $TMT(MeO)^+$ in the rds is the same for both the reactions.

Due to the mechanistic difference revealed here, simple comparison of the reaction rate is difficult between $TMT^{\bullet+}$ (4.5 M^{-3} s^{-1}) and TMT^{2+} (33 M^{-2} s^{-1}). However, by multiplying the former value by the initial concentration of $TMT^{\bullet+}$ (0.5 mM), the higher reactivity of TMT^{2+} is apparent.

Reaction of TMT^{2+} with Py

Next, the reaction of TMT^{2+} with Py was analysed. In this case, the reaction is so fast that the time–decay curves were observed in the Py concentration range of 0.5 to 2.5 mM for the reaction with 0.25 mM TMT^{2+}. Fig. 6 shows the dynamic transformation of absorption spectra in the reaction of TMT^{2+} with Py.

For the decay with time of TMT^{2+} at 701 nm, numerical simulation analysis was also performed as in the previous communication.[7] Although pseudo-reaction order analysis could not be applied in this case, the simulated decay curve fitted all the data obtained at various concentrations of Py. Consequently, the reaction orders of both TMT^{2+} and pyridine were determined to be first. Thus, the rate law is expressed as in eqn. (11).

$$-d[TMT^{2+}]/dt = k[TMT^{2+}][Py] \qquad (11)$$

Together with the reaction orders, the reaction rate, k, in eqn. (11) was determined to be 8.5×10^2 M^{-1} s^{-1}. The rate law of eqn. (11) means that the first encounter of TMT^{2+} and Py is the rds as shown in eqn. (12).

$$TMT^{2+} + Py \xrightarrow[rds]{} TMT(Py)^{2+} \qquad (12)$$

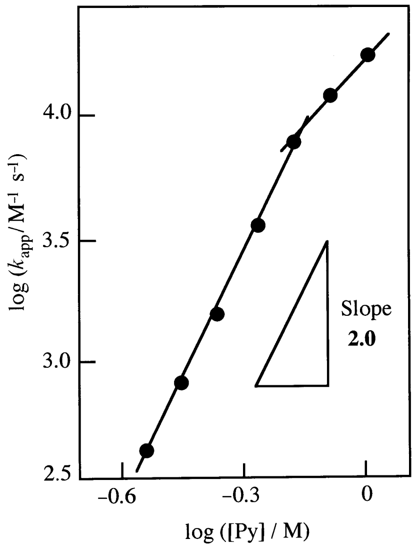

Fig. 7 Dependence of the pseudo-second-order rate constant, k_{app}, on the concentration of Py in the reaction of $TMT^{\bullet+}$ with Py.

In this reaction, a noteworthy feature is that $TMT^{\bullet+}$ was generated in the successive reactions as shown in Fig. 6. Upon increasing the concentration of pyridine, the generation of $TMT^{\bullet+}$ was enhanced in the measured absorption spectra. However, the decay reaction of TMT^{2+} with pyridine was almost complete before the start of the generation of $TMT^{\bullet+}$. Thus, $TMT^{\bullet+}$ is inferred to be generated after the rds [eqn. (12)].

Reaction of $TMT^{\bullet+}$ with Py

Similarly, the reaction of $TMT^{\bullet+}$ with Py was analysed. It was found that this reaction was second-order in $TMT^{\bullet+}$. Fig. 7 shows the plot of log k_{app} *vs.* log [Py]. From this relationship, the reaction order of Py was determined to be second at lower concentrations of Py [eqn. (13)]. However, at higher concentrations, the slope changed so as to indicate a first-order dependence [eqn. (14)] rather than second.

$$-d[TMT^{\bullet+}]/dt = k[TMT^{\bullet+}]^2[Py]^2 \qquad (13)$$

$$-d[TMT^{\bullet+}]/dt = k[TMT^{\bullet+}]^2[Py] \qquad (14)$$

Thus, for the reaction of $TMT^{\bullet+}$ with Py, eqns. (15)–(17) can be proposed, in which the rds is susceptible to the concentration of Py. If eqn. (15) is the rds, the reaction order of Py is first [eqn. (14)], and if eqn. (16) is the rds, then the reaction order is second [eqn. (13)].

In the previous report using a channel-flow method, the first-order dependence of [Py] was reported for this reaction.[11] Also, for the reaction of $TH^{\bullet+}$ with Py, a mechanism was reported in which the second step is the rds.[10] On the basis of the rate law of eqn. (13), the rate constant, k, is estimated to be 3.0×10^4 M^{-3} s^{-1} by extrapolating [Py] to 1.0 M; on the basis of eqn. (14), k is 1.6×10^4 M^{-2} s^{-1}.

$$TMT^{\bullet+} + Py \rightleftharpoons TMT(Py)^{\bullet+} \qquad (15)$$

$$TMT(Py)^{\bullet+} + TMT^{\bullet+} \longrightarrow TMT(Py)^{2+} + TMT \qquad (16)$$

$$TMT(Py)^{2+} + Py \longrightarrow TMT(Py)_2{}^{2+} \qquad (17)$$

In the reactions with Py of both $TMT^{\bullet+}$ and TMT^{2+}, the isolated product was TMT(O), which is similar to the reactions with MeOH. It is thus inferred that TMT(O) is produced after the rds in solution or in the work-up processes.

Table 1 Results of the kinetic analysis of the reactions of $TMT^{\bullet+}$ and TMT^{2+} (Ox) with MeOH and Py (Nu)[a]

Ox	Nu	Concentration range of Nu/M	Reaction order Ox	Reaction order Nu	Rate constant
$TMT^{\bullet+}$	MeOH	3.0–7.0	2	2	4.5 M^{-3} s^{-1}
	Py	0.1–0.6	2	2	3.0×10^4 M^{-3} s^{-1}
	Py	0.6–1.0	2	1	1.6×10^4 M^{-2} s^{-1}
TMT^{2+}	MeOH	0.2–1.0	1	2	3.3×10 M^{-2} s^{-1}
	Py	$0.2–2.5 \times 10^{-3}$	1	1	8.5×10^2 M^{-1} s^{-1}

[a] Based on each rate law of $-d[Ox]/dt = k[Ox]^p[Nu]^q$, the rate constants were determined by extrapolation to [Nu] = 1.0 M or by direct simulation.

Comparison of the reactivities of TMT^{2+} and $TMT^{\bullet+}$

The results obtained above show that the reaction mechanisms are quite different for the reactions of TMT^{2+} and $TMT^{\bullet+}$ as well as for the reactions with MeOH and Py.

Table 1 summarizes the reaction orders and the reaction rates of the analysed reactions. Because the rate laws are different in the respective cases, it is difficult to compare the reactions directly. However, the changes in the reactivity can be estimated by multiplying the concentrations. Also, the measured concentration range would be also a measure of the reactivity. Thus, as a whole, the higher reactivity of TMT^{2+} than $TMT^{\bullet+}$ is confirmed as well as its higher reactivity toward Py than toward MeOH. As a remarkable mechanistic difference between the reactions of TMT^{2+} and $TMT^{\bullet+}$, it is pointed out that the number of pre-equilibria before the rds is not the same.

The reactions of $TMT^{\bullet+}$ were found to proceed *via* two or three steps including the electron transfer of another $TMT^{\bullet+}$ to generate TMT before the rds as indicated by the second-order dependence on $[TMT^{\bullet+}]$. This type of rate law has been reported in the reactions of other cation radicals with nucleophiles.[1–3] On the other hand, in the case of TMT^{2+}, the rds is the first or the second step of the reactions; *i.e.* the unstable cationic intermediate seems to be formed directly, not by electron transfer.

Therefore, while promotion of the first attack, caused by the excessive charge in the dicationic state,[8] would be a significant factor for the higher reactivity of TMT^{2+}, mechanisms in which TMT^{2+} is easily accessible to the rds also could also explain the higher reactivity of TMT^{2+} compared with $TMT^{\bullet+}$.

In addition, the difference in the apparent decay rate between $TMT^{\bullet+}$ and TMT^{2+} is more noticeable in the reactions with Py than in those with MeOH as recognized from the measured concentration ranges of the nucleophiles in Table 1. This difference is assumed to come from the change in the mechanism as represented in eqns. (3), (4) and in eqn. (12) because the ease of initial attack caused by the excessive charge at the sulfur centers should be similar in both reactions. In the reaction with Py, the faster reaction rate of TMT^{2+} is expected to come from the reaction mechanism in which direct attack is the rds [eqn. (12)], while the reaction with MeOH involves two steps [eqns. (3), (4)].

Substituent effects of pyridine derivatives on reactions with TMT^{2+} and $TMT^{\bullet+}$

In order to clarify the influence on the reactivity of the number of steps to the rds, we analysed the reactions of TMT^{2+} and $TMT^{\bullet+}$ with various pyridine derivatives (XPy). The results are summarized in Tables 2 and 3, for TMT^{2+} and $TMT^{\bullet+}$, respectively.

It is known that the influence of substituents on the pyridine derivatives manifests itself as steric and electronic effects. For example, in the reactions of cation radicals derived from 9-phenylanthracene ($9XA^{\bullet+}$), the reaction rates with 4-methylpyridine (4MPy) are faster and those with 4-cyanopyridine (4CPy) are slower, than those with Py reflecting the electronic effect of the substituents in the 4-position.[17] Also, substituents on the 2- and 6-positions cause deceleration of the reactions due to a steric effect that is concurrent with the electronic effect.[17] While these results have been obtained in the reactions of the cation radicals, the reaction mechanism of $9XA^{\bullet+}$ with Py is similar to that of TMT^{2+} in the present study. This is because the first encounter step governs the reaction rate in both reactions.

Table 2 Results of the kinetic analysis of the reactions of TMT^{2+} with pyridine derivatives

XPy[a]	Concentration range of XPy/mM	Reaction order TMT^{2+}	Reaction order XPy	Log (k/M^{-1} s^{-1})
Py	0.2–2.5	1	1	2.9
4MPy	0.2–1.3	1	1	5.1
4CPy	0.2–1.3	1	1	1.0
2MPy	0.2–2.5	1	1	3.4
24MPy	0.2–2.5	1	1	3.7
26MPy	0.2–2.5	1	1	3.7
246MPy	0.2–2.5	1	1	3.9
2EPy	0.7–2.5	1	1	2.5
2PPy	0.7–2.5	1	1	2.5

[a] Abbreviations: Py = pyridine, 4MPy = 4-methylpyridine, 4CPy = 4-cyanopyridine, 2MPy = 2-methylpyridine, 24MPy = 2,4-dimethylpyridine, 26MPy = 2,6-dimethylpyridine, 246MPy = 2,4,6-trimethylpyridine, 2EPy = 2-ethylpyridine, 2PPy = 2-phenylpyridine.

Therefore, the results in Table 2 seem to be most reasonable, taking into account both the electronic and steric effects of the substituents. Because the reaction rates are governed by the first interaction between TMT^{2+} and XPy, it can be concluded that the substituent effects manifested themselves as both steric and electronic effects. The differences in the reaction rates due to the substituents on the 4-position, $-CH_3$, –H and –CN, were more significant in the present reaction compared with the reported ones.[17] In addition, significant steric hindrance was observed in the case of the present 2- and 6-substituted derivatives.

In contrast, in the reactions of $TMT^{\bullet+}$, the occurrence of a substituent effect changes as shown in Table 3. While the reaction order of Py in the reaction with $TMT^{\bullet+}$ was complicated (as shown in Fig. 7), apparent changes in the reaction order only arose in the reaction with 4MPy. It is expected that this difference is caused by the electron-donating methyl substituent, which changes the rds to eqn. (16). Besides this change, the most significant feature was the occurrence of a steric effect in the 2- and 6-positions. The decay of $TMT^{\bullet+}$ in the presence of 2-methylpyridine, 2,4-dimethylpyridine, 2,6-dimethylpyridine or 2-methylpyridine was much faster than that with Py, and, furthermore, than that with 4MPy. Thus, in the reactions of $TMT^{\bullet+}$ with XPy, the steric effect is concluded to be very small, compared with the reactions of TMT^{2+}. This result is in accord with a reaction mechanism in which there are several steps before the rds. The complex aspect of the mechanism is inferred to have changed the appearance of a substituent effect in a different manner from in the case of TMT^{2+}.

While the substituent effects on $TMT^{\bullet+}$ have been discussed above by comparing mechanistically those on TMT^{2+}, it is also

Table 3 Results of the kinetic analysis of the reactions of $TMT^{\bullet+}$ with pyridine derivatives

		Reaction order		
XPy[a]	Concentration range of XPy/M	TMT^{2+}	XPy	Log *k*
Py	0.1–0.6	2	2	4.5[b]
Py	0.6–1.0	2	1	4.2[c]
4MPy	0.025–0.25	2	1	3.9[c]
2Mpy	0.025–0.25	2	2	5.0[b]
24MPy	0.025–0.25	2	2	5.6[b]
26MPy	0.025–0.25	2	2	5.5[b]
2EPy	0.05–0.2	2	2	5.5[b]

[a] Abbreviations: Py = pyridine, 4MPy = 4-methylpyridine, 2MPy = 2-methylpyridine, 24MPy = 2,4-dimethylpyridine, 26MPy = 2,6-dimethylpyridine, 2EPy = 2-ethylpyridine. [b] Units of the rate constant: $M^{-3}\ s^{-1}$. [c] Units of the rate constant: $M^{-2}\ s^{-1}$.

expected that the positive charges on TMT, *i.e.*, $TMT^{\bullet+}$ or TMT^{2+}, change the way XPy approaches for reaction.

Conclusion

The differences in the reactivity of the cation radical and dication have been clarified in their reactions with MeOH, Py and XPy in the case of TMT, in particular, in the light of their reaction mechanisms. While a simple comparison was difficult because of the changes in reaction mechanism depending on the oxidation states, *i.e.*, $TMT^{\bullet+}$ and TMT^{2+}, and on the nucleophiles, the higher reactivity of TMT^{2+} was confirmed in reactions with all the nucleophiles.

In the present results, in addition to the excessive charge in the dicationic state, the change in mechanism is concluded to be a significant factor in bringing about the higher reactivity of TMT^{2+}. By proceeding directly to the rds, it is expected that the overall reactivity of TMT^{2+} is increased significantly.

The present results indicate that there is a remarkable mechanistic difference in the reaction mechanisms also between the reactions with MeOH and with Py. Parker and Tilset reported the superacid properties of dications in solution.[5] For proton-releasing nucleophiles such as MeOH, it is inferred that the reaction proceeds by proton abstraction from the dicationic adduct (TMT^{+}–$MeOH^{+}$). In contrast, in the cases of Py and XPy, because the dication would be stabilized by the formation of a dicationic adduct,[5] it seems that TMT^{+}–Py^{+} is formed in the rds. However, the reaction pathway after the rds is uncertain because only TMT(O) was isolated in all the reactions.

References

1 K. Yoshida, *Electrooxidation in Organic Chemistry*, John Wiley & Sons, Inc., New York, 1984.
2 O. Hammerich and V. D. Parker, in *Advances in Physical Organic Chemistry*, ed. V. Gold and D. Bethell, Academic Press, London, 1984, Vol. 20, p. 55.
3 V. D. Parker, *Acc. Chem. Res.*, 1984, **17**, 243.
4 K. Yasukouchi, I. Taniguchi, H. Yamaguchi, J. Ayukawa, K. Ohtsuka and Y. Tsuruta, *J. Org. Chem.*, 1981, **46**, 1679.
5 V. D. Parker and M. Tilset, *J. Am. Chem. Soc.*, 1988, **110**, 1649.
6 V. D. Parker, M. Pedersen and B. Reitstoen, *Acta Chem. Scand.*, 1993, **47**, 560.
7 M. Oyama, T. Sasaki and S. Okazaki, *J. Electroanal. Chem.*, 1997, **420**, 1.
8 H. Bock, A. Rauschenbach, K. Ruppert and Z. Havlas, *Angew. Chem., Int. Ed. Engl.*, 1991, **30**, 714.
9 M. Oyama, S. Okazaki and T. Nagamura, *Vib. Spectrosc.*, 1991, **1**, 329.
10 J. F. Evans and H. N. Blount, *J. Org. Chem.*, 1977, **42**, 976.
11 F. Prieto, M. Oyama, B. A. Coles, J. A. Alden, R. G. Compton and S. Okazaki, *Electroanalysis*, 1998, **10**, 685.
12 M. Oyama, K. Nozaki and S. Okazaki, *Anal. Chem.*, 1991, **63**, 1387.
13 M. Oyama, M. Yamanuki, T. Sasaki and S. Okazaki, *J. Chem. Soc., Perkin Trans. 2*, 2000, 1745.
14 T. Weiβ and G. Klar, *Liebigs Ann. Chem.*, 1978, 785.
15 A. W. Addison, T. H. Li and L. Weiler, *Can. J. Chem.*, 1977, **55**, 766.
16 M. Oyama, K. Nozaki, T. Nagaoka and S. Okazaki, *Bull. Chem. Soc. Jpn.*, 1990, **63**, 33.
17 B. Reitstöen and V. D. Parker, *J. Am. Chem. Soc.*, 1991, **113**, 6954.